THE JOURNAL OF PHYSICAL CHEMISTRY Letters

LETTER

pubs.acs.org/JPCL

Applicability of Birth−Death Markov Modeling for Single-Molecule Counting Using Single-Walled Carbon Nanotube Fluorescent Sensor Arrays

Zachary W. Ulissi, Jingqing Zhang, Ardemis A. Boghossian, Nigel F. Reuel, Steven F. E. Shimizu, Richard D. Braatz, and Michael S. Strano*

Department of Chemical Engineering, Massachusetts Institute of Technology, 77 Massachusetts Avenue, Cambridge, Massachusetts 02139, United States

Supporting Information

ABSTRACT: In recent work, we have shown that $d(AT)_{15}$ DNA-wrapped single-walled carbon nanotubes (SWNTs) are able to detect the adsorption and desorption of single molecules of nitric oxide (NO) from the surface by quenching of the near-infrared fluorescence (Zhang et al. J. Am. Chem. Soc. 2011, 133, 567−581). A central question is how to estimate the local concentration from stochastic dynamics for these types of sensors. Herein, we employ an exact solution to the birth−death Markov model to estimate the local analyte concentration from the stochastic dynamics. Conditions are derived for the intrinsic variance displayed by identical sensor elements, and the homogeneity of the environment is assessed by comparing experimental sensor-to-sensor variance with this limit. We find that $d(AT)_{15}$ DNA-wrapped SWNTs demonstrate variances that are close to the idealized limit at relatively high NO concentrations (19.4 μM). At 780 nM, the sensor-to-sensor variance is approximately double the idealized value, indicating marginal variation in the SWNT array. An NO adsorption coefficient of 2.6×10^{-4} [μM^{-1}] is identified, and we outline how to predict the local analyte concentration from the sensor dynamics.

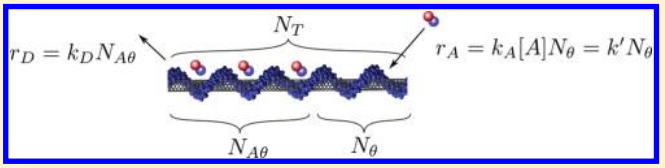

SECTION: Nanoparticles and Nanostructures

An important development in nanotechnology is the emergence of sensor transducers capable of single-molecule resolution at room temperature. SWNTs alone account for at least three sensor types capable of this important property. One sensor type is an electrically contacted field effect transistor (FET) with a single electrochemically induced catalytic defect, inducing a defection in the channel current in response to reactions at the defect site.[1−3] A second sensor type uses the interior of the SWNT as a nanopore for Coulter detection of single cations.[4] A third sensor type consists of a near-infrared fluorescent semiconducting SWNT where adsorption and desorption of a fluorescence quencher cause discretized and stochastic fluctuations of the intensity from the single nanotube. We have developed several near-infrared fluorescent SWNT sensors selective for glucose,[5−8] DNA,[9−12] ATP,[13] H_2O_2,[14,15] and recently NO.[16,17] For H_2O_2 and NO, we first introduced the idea of a selective sensor interface able to count single analyte molecules, following the pioneering experiments of Cognet and Weismann demonstrating stochastic fluorescence quenching of SWNT excitons.[18] A central challenge in the theory of these single-molecule sensors is how to relate intensity fluctuations to the local analyte concentration of interest and/or its flux to the sensor. We have used recently, without rigorous proof, a birth−death Markov model to accomplish this. This Letter develops a mathematical test for the agreement of molecular adsorption dynamics for this Markov process.

When molecules bind to the surface of a SWNT, the fluorescence is partially quenched, resulting in a step decrease in intensity. Similarly, the intensity increases when molecules unbind from the surface. By counting the transient change in the number of step changes in intensity, the number of adsorption and desorption events, the total number of adsorbed molecules, and the incident flux can be estimated.

Exciton quenching by adsorbed analyte molecules limits the number of observable adsorption and desorption states. For a typical SWNT sensor, the number of states will be about 10, based on a mean nanotube length of 1 μm and an estimated exciton diffusion length of 100 nm.[17] More detailed physical models of exciton dynamics propose that the diffusion length is limited by pre-existing or static defects,[19] but the analysis of adsorption and desorption kinetics in this work applies to these physical models as well. Due to this small number of observable states, adsorption and desorption events will be stochastic, which results in a deviation in the observed number of bound analyte molecules from the number predicted by the continuum approximation or average sensor. These stochastic deviations can cause the apparent reaction rates to be different for various SWNTs

Received: April 29, 2011
Accepted: June 2, 2011
Published: June 02, 2011

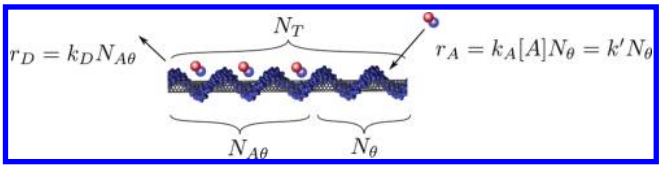

Figure 1. Model of the SWNT sensor, with rates of chemical adsorption and desorption.

even when the underlying rates are the same (i.e., the nanotubes are chemically identical).

Each sensor is modeled as a surface with a fixed total number of adsorption sites N_T, as shown in Figure 1. The most recent theory of exciton dynamics on a pristine SWNT assumes that there is no limit to the number of adsorption/quenching events, and these can happen anywhere along the length.[19] In practice, it is believed that either the matrix or tethering chemistry divides the SWNT into isolated segments, each of which can be quenched completely through an adsorption event, in agreement with recent experimental studies.[14−17] Further work is necessary to reconcile these two physical models.

Free analyte molecules in the surrounding liquid A (concentration, $[A]$ M) are assumed to bind to an empty nanotube segment, θ, (number, $N_\theta \in [0,N_T]$) to form bound molecules (number, $N_{A\theta} \in [0,N_T]$) through the reversible reaction

$$A + \theta \underset{k_D}{\overset{k_A}{\rightleftharpoons}} A\theta$$

where k_A $[M^{-1}\,s^{-1}]$ and k_D $[s^{-1}]$ are coefficients for adsorption and desorption, respectively. Although these coefficients are often constant, they could change with external stimuli such as temperature and thus could be time-dependent.

Assuming mass action kinetics, the net adsorption rate in the continuum limit is

$$r = r_A - r_D = k_A[A]\overline{N}_\theta - k_D\overline{N}_{A\theta} = k'_A(t)\overline{N}_\theta - k_D\overline{N}_{A\theta} \quad (1)$$

where rates are given in $s^{-1}$and $k'_A(t) = k_A[A(t)]$ $[s^{-1}]$ is a pseudo-first-order rate coefficient for when the concentration of A in the liquid phase is not significantly affected by the individual adsorption/desorption event. If the reaction rate is not first order in liquid concentration, which is a plausible scenario at low concentrations, the definition for the pseudo-first-order constant can be adjusted (e.g., $k'_A = k_A[A]^{1/2}$) without affecting any other results. If the reaction rate is not first order in the number of sites, the stochastic solution presented below will not be applicable, and a more complicated stochastic solution will be necessary. A final algebraic relation can be obtained through a balance on the number of adsorption sites, $N_T = N_\theta + N_{A\theta}$. The continuum solution is found by solving the appropriate ordinary differential equation

$$\frac{d\overline{N}_{A\theta}}{dt} = r = k'_A\overline{N}_\theta - k_D\overline{N}_{A\theta} = k'_A(N_T - \overline{N}_{A\theta}) - k_D\overline{N}_{A\theta} \quad (2)$$

With initially empty ($N^{t=0}_{A\theta} = 0$) surface and constant rate coefficients (denoted by E), the analytical solution is

$$\tilde{N}^E_{A\theta}(t) = \frac{\overline{N}^E_{A\theta}(t)}{N_T} = \frac{1 - \exp[-(k'_A + k_D)t]}{1 + k_D/k'_A} \quad \text{for } \overline{N}^0_{A\theta} = 0 \quad (3)$$

The corresponding solution for an initially full ($N^0_{A\theta} = N_T$) surface is included in the Supporting Information. For rate coefficients that change over time (due to changing analyte concentration or temperature), alternative analytic solutions to eq 2 can be derived by applying the integrating factor $\exp[k'_A(t) + k_D(t)]$.

How does the individual sensor-to-sensor response vary within a collection of sensors? This variation can be due to the chemical or physical environment or due to imperfections on the SWNTs themselves. We call this type of variation extrinsic. Alternatively, because the sensors count single molecules, we expect some intrinsic stochastic variation among even perfectly identical sensors. One important question to ask is if the variances in the sensor responses are within this intrinsic limit (indicating that the sensors are nearly identical) or if the variance is much larger (perhaps due to a spatially inhomogeneous environment).

This question can be addressed by analysis of the stochastic chemical master equation (CME), which is a system of differential equations that describes the probability of each possible state in the system at each time t (see Supporting Information). For the birth−death model, the SWNT sensor states[17] can be characterized by the number of adsorbed molecules, resulting in $N_T + 1$ total states, each with a probability $\Pr(N_{A\theta} = i) \in [0,1]$. Solving the CME directly for the birth−death model requires the solution of $N_T + 1$ ordinary differential equations, which is feasible for moderate N_T but not convenient. Instead, analytical solutions for probability distributions are sought and verified with the CME.

Probability distributions for the number of empty (N_θ) and bound ($N_{A\theta}$) sites are derived instead of solving the standard CME. This first-order adsorption/desorption system is essentially identical to the isomerization example (example 5.2) in ref 20, and for convenience, the derivation is included in the Supporting Information. The number of adsorbed molecules $N_{A\theta}$ at a time t is a random variable distributed as a binomial with number of trials N_T and probability $\tilde{N}_{A\theta}$ from solving the continuum problem in eq 2 with the appropriate initial condition for the average fraction of initially occupied sites (eq 3)

$$N_{A\theta} \sim \mathrm{Bin}(N_T, \tilde{N}_{A\theta}(t))$$
$$\Pr(N_{A\theta} = i) = \binom{N_T}{i}(\tilde{N}_{A\theta}(t))^i(1 - \tilde{N}_{A\theta}(t))^{N_T - i} \quad (4)$$

When the initial state is an entirely empty ($N^0_{A\theta} = 0$) or full ($N^0_{A\theta} = N_T$) sensor and the rate coefficients are constant, the initial binomial distribution becomes deterministic and

$$\Pr(N_{A\theta} = i | N_{A\theta}(t = 0) = 0) = \begin{cases} \delta_{i,0} & \text{for } t = 0 \\ \binom{N_T}{i}(\tilde{N}^E_{A\theta}(t))^i(1 - \tilde{N}^E_{A\theta}(t))^{N_T - i} & \text{for } t \geq 0 \end{cases} \quad (5)$$

where $\delta_{i,j}$ is the Kronecker delta function (1 if $i = j$ and 0 otherwise) and $\tilde{N}^E_{A\theta}(t)$ is the continuum solution in eq 3. The analagous probability distribution starting with a full sensor ($\tilde{N}^F_{A\theta}(t)$) is included in the Supporting Information. The solution for an initially empty surface ($N^0_{A\theta} = 0$) at several times is shown in Figure 2, along with sample experimental distributions from previous studies.[17] Reasonable agreement is seen between the birth−death model and the experimental data. Less agreement is seen at small times, where transient effects from introducing

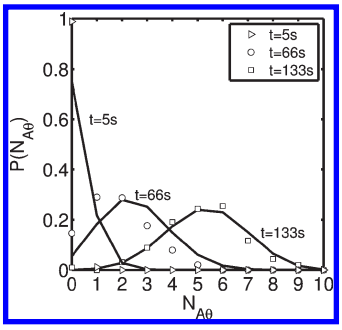

Figure 2. Plot of the probability distribution over time for the binomial solution (solid lines) as well as for representative experimental data (open shapes) from a previous study for a SWNT sensor exposed to 19.4 μM nitric oxide.[17] The parameters used in the model are fits with the exact numerical MLE, with values $k'_A = (5.5 \pm 0.5) \times 10^{-3}$ s^{-1} and $k_D = (3.9 \pm 2.1) \times 10^{-4}$ s^{-1}.

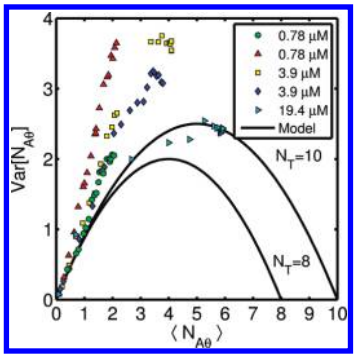

Figure 3. Comparison of the birth−death model with experimental data for five arrays of SWNT sensors exposed to solutions of varying NO concentration from a previous study.[17] Model results were obtained by plotting the variance, $N_T\tilde{N}_{A\theta}(1 - \tilde{N}_{A\theta})$ versus the mean, $N_T\tilde{N}_{A\theta}$, with two values of N^T.

analyte into the experimental system may play a role. For an initial state with an arbitrary number of bound sites $N^0_{A\theta}$, the distribution of the number of bound molecules will simply be the convolution ($*$) of the distributions for the initially empty and full portions[20]

$$N_{A\theta} \sim \mathrm{Bin}(N^0_{A\theta}, \tilde{N}^F_{A\theta}(t)) * \mathrm{Bin}(N_T - N^0_{A\theta}, \tilde{N}^E_{A\theta}(t)) \qquad (6)$$

With knowledge of the full distribution as a function of time, the time-dependent properties of the distribution can be calculated by substituting values into known formulas for the binomial distribution. An initially empty surface with constant rate coefficients (as is typical for previous experiments[17]) has mean and variance

$$\langle N_A \rangle(t) = N_T p = N_T \left(\frac{1 - \exp[-(k'_A + k_D)t]}{1 + k_D/k'_A} \right)$$

$$\mathrm{Var}[N_A](t) = \sigma^2 = N_T p(1-p)$$

$$= N_T \left(\frac{k_D/k'_A + (1 - k_D/k'_A)\exp[-(k'_A + k_D)t]}{(1 + k_D/k'_A)^2} \right) \qquad (7)$$

This suggests a characteristic relationship between the variance in measurements of the number of adsorbed molecules and the average number of adsorbed molecules for the birth−death process. Figure 3 shows the observed relationship between the mean and variance of the number of occupied sites for experimental SWNT sensor arrays at various analyte concentrations compared to the birth−death model with varying numbers of sites. The model assumes that all sensors have identical properties, even though this is probably not the case experimentally. Thus, the modeled stochastic variance forms a lower bound on the variance observed in experimental processes that follow this simple birth−death model, assuming identical properties for all sensors (i.e., there will be more sensor-to-sensor variation if sensor properties are also varied). An observed variance much larger than this characteristic value would indicate either a large amount of experimental error, variations in the underlying parameters, or a breakdown with the birth−death model. The model with $N_T = 10$ provides a good fit to the high NO concentration data. Lower NO concentrations behave similarly for low coverage but exhibit increased variance at higher coverage, which may be an indication of environmental inhomogeneity (lower NO concentrations should take more time to diffuse uniformly throughout the liquid film, for example).

Applications to Stochastic Parameter Fitting. Knowing the exact probability distribution for the system allows for straightforward fitting of model parameters for an array of SWNT sensors instead of analyzing sensors individually.[17,21,22] The likelihood of a set of parameters θ given a series of system measurements is defined[21] as $L(\theta) = \Pr(x_1,x_2,...,x_n)$. The maximum likelihood estimator (MLE) is obtained by identifying the set of parameters θ that maximizes the likelihood. In previous studies of an array of SWNT sensors, adsorption and desorption coefficients in the birth−death model were estimated by averaging parameters obtained by applying the MLE to each trace individually. Here, this method is shown to yield inaccurate parameter fits. The exact MLE can be calculated for the entire sensor array simultaneously using the above analytical results from eq 6.

The exact birth−death MLE for a SWNT sensor array can be calculated to provide substantially more accurate results than previous methods. When multiple sensors are observed independently, each measurement will be dependent on the data in its own trace but independent of the measurements in all other traces. Thus, the likelihood function, $L(\theta)$ for N_Q independent SWNT sensors with measurements x^j_i, $i \in [1,N_j]$, $j \in [1,N_Q]$ (each measurement composed of the number of bound molecules $N^{i,j}_{A\theta}$ at times $t^{i,j}$) is

$$L(\theta) = \prod_{j=1}^{N_Q} [\Pr(x^j_1|\theta) \prod_{i=2}^{N_j} \Pr(x^j_i|x^j_{i-1},\theta)]$$

$$= \prod_{j=1}^{N_Q} [\prod_{i=2}^{N_j} \Pr(x^j_i|x^j_{i-1},\theta)]$$

$$\log L(\theta) = \sum_{j=1}^{N_Q} [\log \Pr(x^j_1|\theta) + \sum_{i=2}^{N_j} \log \Pr(x^j_i|x^j_{i-1},\theta)] \qquad (8)$$

where $\Pr(x^j_1|\theta)$ is the probability of the first measurement of $N_{A\theta}$ for the jth sensor and $\Pr(x^j_i|x^j_{i-1},\theta)$ is the probability of the ith measurement of $N_{A\theta}$ for the jth sensor given the measurement immediately preceding it in time. $\Pr(x^j_1|\theta)$ is unity as our experiments started with clean SWNTs free of analyte molecules. Calculating likelihoods usually involves the multiplication of many small numbers; therefore, the log-likelihood is calculated as a sum instead. Because the full

probability distribution is known, the likelihood in eq 8 can be directly calculated using the exact results of eq 6, with $\Pr(x_i^j|x_{i-1}^j,\theta) = \Pr(N_{A\theta}^{t=t_i^j-t_{i-1}^j} = N_{A\theta}^{i,j}|N_{A\theta}^{t=0} = N_{A\theta}^{i-1,j})$ and parameters $\theta = (k'_A,k_D)$. The problem is computationally tractable because each probability evaluation is simply an algebraic evaluation. The Matlab constrained optimization algorithm **fmincon** is used to minimize the log-likelihood over all positive values with initial guesses based on the previous analytical method above.

Data for the number of adsorbed molecules on SWNT sensors can be analyzed using an analytical MLE for the birth−death model[17,22]

$$\hat{k}'_A = \frac{B_t}{N_T t - S_t} \qquad \hat{k}_D = \frac{D_t}{S_t} \tag{9}$$

where B_t is the number of adsorption events (births), D_t is the number of desorption events (deaths), t is the total observation time, and $S_t = \int_0^t N_{A\theta}\, dt$ is the integrated number of adsorbed molecules. Our previous study derived this equation for a single SWNT sensor and fit parameters by averaging the MLE parameters estimates for each tube.[17] The analytical MLE for a collection of SWNT sensors observed at uniform time increments Δt was calculated by analytically equating $\partial \log L/\partial k'_A = \partial \log L/\partial k_D = 0$, expanding in powers of Δt, and solving for $\hat{k}'_A$ and $\hat{k}_D$. Keeping the zeroth- and first-order terms, corresponding to continuously observed SWNTs, yielded eq 9, except that B_t, S_t, D_t, and t were summed for all sensors

$$\lim_{\Delta t \to 0} \hat{k}'_{A,MLE} = \frac{\sum B_t^j}{N_T \sum t^j - \sum S_t^j} \neq \left\langle \frac{B_t^j}{N_T t^j - S_t^j} \right\rangle$$
$$\lim_{\Delta t \to 0} \hat{k}_{D,MLE} = \frac{\sum D_t^j}{\sum S_t^j} \neq \left\langle \frac{D_t^j}{S_t^j} \right\rangle \tag{10}$$

The remaining terms ($O[\Delta t]^2$ and higher) represent deviations in the exact MLE eq 8 from the continuous observation limit. The magnitude of higher-order contributions was calculated for previous experiments[17] to be less than 3% of the zeroth- and first-order contributions. Note that averaging the MLE estimates for individual traces, indicated as the bracketed terms, yields incorrect parameter estimates.

The confidence bounds on the parameter estimates provided by eq 10 can be estimated by calculating the bounds in the continuous observation limit ($\Delta t = 0$). The 95% error bounds can be derived by linearizing the log-likelihood function around the MLE-fitted parameter vector $\theta = (k'_A,k_D)$ and using a χ^2 test with two free parameters

$$(\theta - \hat{\theta})^T \nabla_{\theta\theta}[-\log L](\theta - \hat{\theta}) \leq \chi_2^2(0.95) \tag{11}$$

The middle term $\nabla_{\theta\theta}[-\log L]$ can be calculated exactly for the continuous observation limit

$$\lim_{\Delta t \to 0} \nabla_{\theta\theta}[-\log L] = \begin{pmatrix} \frac{N_{ads}^{obs}}{\hat{k}'^2_A} & 0 \\ 0 & \frac{N_{des}^{obs}}{\hat{k}_D^2} \end{pmatrix} \tag{12}$$

where N_{ads}^{obs} and N_{des}^{obs} are the number of adsorption and desorption events observed for all sensors. Because the two parameters are uncoupled in this limit (covariances are zero), the 95% confidence intervals can be easily calculated

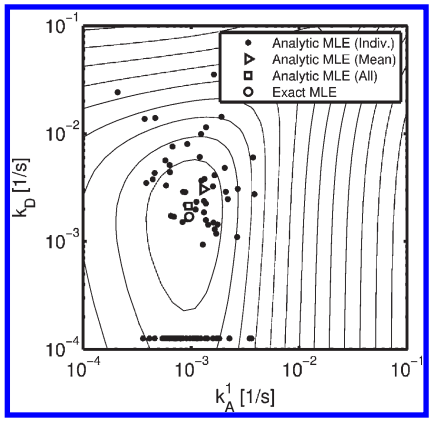

Figure 4. Comparison of four different methods for fitting rate coefficients to data from a previous study for a SWNT sensor array exposed to a 0.78 μM nitric oxide solution. Methods include (filled circles) applying the analytic MLE to individual sensors, (open triangle) averaging the results of the analytic MLE applied to each trace, (open square) applying the analytic MLE to all traces, and (open circle) using the exact MLE based on the full solution. When no desorption events are observed, the MLE estimate yields $k_D = 0$, and these points are included at the bottom.

$$\hat{k}'_A - \hat{k}'_A\sqrt{\frac{\chi_2^2(0.95)}{N_{ads}^{obs}}} \leq k'_A \leq \hat{k}'_A + \hat{k}'_A\sqrt{\frac{\chi_2^2(0.95)}{N_{ads}^{obs}}}$$
$$\hat{k}_D - \hat{k}_D\sqrt{\frac{\chi_2^2(0.95)}{N_{des}^{obs}}} \leq k_D \leq \hat{k}_D + \hat{k}_D\sqrt{\frac{\chi_2^2(0.95)}{N_{des}^{obs}}} \tag{13}$$

This result explains the variations in observed coefficients that we reported previously as rate constant histograms[17] and gives a bound for the observation time needed to obtain accurate parameter estimates. In order to achieve 10% accuracy in either the adsorption or desorption coefficient, roughly 600 event observations are required. The rate constant histograms reported previously are not rigorous because they convolute the intrinsic and extrinsic variances for the collection of sensors. However, the above methods require the assumption of a collective concentration above the sensor array and do not allow for an examination of single sensor dynamics, even though this limit is the most compelling for nanosensor applications.

The fitting capability of the new exact MLE was compared to the previous method for individual SWNTs using results for SWNT nanotube sensors exposed to aqueous solutions at a NO concentration of 0.78 μM,[17] shown in Figure 4. Contour lines represent the true log-likelihood surface, which would be unfeasible to calculate without the new method. The analytical MLE was first applied to the trace for each nanotube, resulting in a range of fitted parameters previously reported as rate coefficient histograms. Two approximate methods for calculating the rate coefficients using all of the data were considered as well, (a) averaging the parameters obtained using the analytical MLE on each sensor as in ref 17 and (b) applying the continuous observation limit analytical MLE to all of the traces simultaneously (summing observation times, births, deaths, and sites for all sensors). Finally, the exact numerical MLE was calculated by optimizing the log-likelihood function. The continuous observation limit MLE was not quite equal to the true MLE due to the $O[\Delta t]^2$ error. The fit using the new method is $k'_A = (8.2 \pm 1.1) \times 10^{-4}$ [1/s], $k_D = (2.1 \pm 0.47) \times 10^{-3}$ [1/s]. These are lower

dx.doi.org/10.1021/jz200572b | J. Phys. Chem. Lett. 2011, 2, 1690–1694

than the values that we estimated previously from considering single sensor dynamics, $k'_A = 1.2 \times 10^{-3}$ [1/s].[17] The current analysis also provides the quantification of the uncertainty.

The analytical probability distribution for the birth−death model has allowed for the expansion of previously published results for the case where a uniform concentration appears above the sensor array. The intrinsic stochastic impact of the system was derived and used to calculate the experimentally observed[17] sensor-to-sensor variance. The exact solution was also used to improve parameter estimation and provide uncertainty estimates on the fitted parameters. Finally, the more general maximum likelihood estimator presented here in eq 9 will be useful for the interpretation of results from sensors in spatially or temporally inhomogeneous environments. We expect that these tools will be useful for the interpretation of future adsorption/desorption-based stochastic sensors.

■ ASSOCIATED CONTENT

Supporting Information. Derivation of the analytical solution to the birth−death model, as well as the relevant chemical master equation. This material is available free of charge via the Internet at http://pubs.acs.org.

■ AUTHOR INFORMATION

Corresponding Author
*E-mail: strano@mit.edu.

■ ACKNOWLEDGMENT

This work was sponsored by the National Science Foundation. M.S.S. acknowledges support from the Beckman Young Investigator Award from the Beckman Foundation. Z.W.U. acknowledges support from the DOE CSGF program (DOE Grant DE-FG02-97ER25308). A.A.B. acknowledges support from the DOD NDSEG program. N.F.R. acknowledges support from the NSF GRFP program.

■ REFERENCES

(1) Collins, P.; Avouris, P. Multishell Conduction in Multiwalled Carbon Nanotubes. *Appl. Phys. A* **2002**, *74*, 329–332.

(2) Collins, P. G.; Arnold, M. S.; Avouris, P. Engineering Carbon Nanotubes and Nanotube Circuits Using Electrical Breakdown. *Science* **2001**, *292*, 706–709.

(3) Collins, P.; Avouris, P. The Electronic Properties of Carbon Nanotubes. *Contemp. Concepts Condens. Matter Sci.* **2008**, *3*, 49–81.

(4) Lee, C. Y.; et al. Coherence Resonance in a Single-Walled Carbon Nanotube Ion Channel. *Science* **2010**, *329*, 1320–1324.

(5) Barone, P. W.; et al. Modulating Single Walled Carbon Nanotube Fluorescence in Response to Specific Molecular Adsorption. *Electron. Prop. Novel Nanostruct.* **2005**, *786*, 193–197.

(6) Barone, P. W.; et al. Near-Infrared Optical Sensors Based on Single-Walled Carbon Nanotubes. *Nat. Mater.* **2005**, *4*, 86–U16.

(7) Barone, P. W.; Parker, R. S.; Strano, M. S. In Vivo Fluorescence Detection of Glucose Using a Single-Walled Carbon Nanotube Optical Sensor: Design, Fluorophore Properties, Advantages, And Disadvantages. *Anal. Chem.* **2005**, *77*, 7556–7562.

(8) Barone, P. W.; Strano, M. S. Reversible Control of Carbon Nanotube Aggregation for a Glucose Affinity Sensor. *Angew. Chem., Int. Ed.* **2006**, *45*, 8138–8141.

(9) Heller, D. A.; et al. Optical Detection of DNA Conformational Polymorphism on Single-Walled Carbon Nanotubes. *Science* **2006**, *311*, 508–511.

(10) Jeng, E. S.; et al. Hybridization Kinetics and Thermodynamics of DNA Adsorbed to Individually Dispersed Single-Walled Carbon Nanotubes. *Small* **2007**, *3*, 1602–1609.

(11) Jin, H.; et al. Divalent Ion and Thermally Induced DNA Conformational Polymorphism on Single-Walled Carbon Nanotubes. *Macromolecules* **2007**, *40*, 6731–6739.

(12) Jeng, E. S.; et al. Detection of DNA Hybridization Using the near-Infrared Band-Gap Fluorescence of Single-Walled Carbon Nanotubes. *Nano Lett.* **2006**, *6*, 371–375.

(13) Kim, J. H.; et al. A Luciferase/Single-Walled Carbon Nanotube Conjugate for Near-Infrared Fluorescent Detection of Cellular ATP. *Angew. Chem., Int. Ed.* **2010**, *49*, 1456–1459.

(14) Jin, H.; et al. Detection of Single-Molecule H_2O_2 Signalling from Epidermal Growth Factor Receptor Using Fluorescent Single-Walled Carbon Nanotubes. *Nat. Nanotechnol.* **2010**, *5*, 302–U81.

(15) Jin, H.; et al. Stochastic Analysis of Stepwise Fluorescence Quenching Reactions on Single-Walled Carbon Nanotubes: Single Molecule Sensors. *Nano Lett.* **2008**, *8*, 4299–4304.

(16) Kim, J. H.; et al. The Rational Design of Nitric Oxide Selectivity in Single-Walled Carbon Nanotube near-Infrared Fluorescence Sensors for Biological Detection. *Nat. Chem.* **2009**, *1*, 473–481.

(17) Zhang, J.; et al. Single Molecule Detection of Nitric Oxide Enabled by d(AT)15 DNA Adsorbed to Near Infrared Fluorescent Single-Walled Carbon Nanotubes. *J. Am. Chem. Soc.* **2010**, 567–581.

(18) Cognet, L.; et al. Stepwise Quenching of Exciton Fluorescence in Carbon Nanotubes by Single-Molecule Reactions. *Science* **2007**, *316*, 1465–1468.

(19) Harrah, D. M.; Swan, A. K. The Role of Length and Defects on Optical Quantum Efficiency and Exciton Decay Dynamics in Single-Walled Carbon Nanotubes. *ACS Nano* **2010**, *5*, 647–655.

(20) Jahnke, T.; Huisinga, W. Solving the Chemical Master Equation for Monomolecular Reaction Systems Analytically. *J. Math. Biol.* **2007**, *54*, 1–26.

(21) Feigin, P. D. Maximum Likelihood Estimation for Continuous-Time Stochastic-Processes. *Adv. Appl. Probab.* **1976**, *8*, 712–736.

(22) Keiding, N. Maximum Likelihood Estimation in the Birth-and-Death Process. *Ann. Stat.* **1975**, *3* (2), 363–372.